Conformational studies of synthetic lipid A analogues and partial structures by infrared spectroscopy

Klaus Brandenburg [a,*], Shoichi Kusumoto [b], Ulrich Seydel [a]

[a] *Forschungszentrum Borstel, Center for Biomedical Research, Parkallee 10, 23845 Borstel, Germany*
[b] *Department of Chemistry, Graduate School of Science, Osaka University, Toyonaka, Osaka 560, Japan*

Abstract

Synthetic lipid A analogues and partial structures were analyzed and compared with natural hexaacyl lipid A from *E. coli* applying Fourier transform infrared spectroscopy. The investigations comprised (i) the measurement of the $\beta \Leftrightarrow \alpha$ phase transition of the acyl chains via monitoring of the symmetric stretching vibration of the methylene groups, (ii) an estimation of the supramolecular aggregate structures evaluating vibrations from the interface like ester carbonyl and applying theoretical calculations (iii) a determination of the inter- and intramolecular conformations monitoring functional groups from the interface and the diglucosamine backbone (ester carbonyl, phosphate). The phase transition temperature T_c was found to be nearly a linear function of the number of acyl chains for most bisphosphoryl compounds indicating comparable packing density, whereas the deviating behaviour of some samples indicated a higher packing density. From the determination of the supramolecular aggregate structures (cubic, H_{II}) of natural hexaacyl lipid A by X-ray small-angle diffraction, the existence of the same aggregate structures also for the synthetic hexaacyl lipid A was deduced from the nearly identical thermotropism of the ester carbonyl band. From this, a good approximation of the supramolecular structures of all synthetic samples was possible on the basis of the theory of Israelachvili. The analysis of the main phosphate band, together with that of the T_c data and former colorimetric results, allowed the establishment of a model of the intermolecular conformations of neighbouring lipid A/LPS molecules. The biological relevance of the findings is discussed in terms of the strongly varying biological activity (between high and no activity) of the samples. © 1997 Elsevier Science B.V.

1. Introduction

Lipopolysaccharides (LPS), the endotoxins of gram-negative bacteria, consist of an oligo- or poly-saccharide chain covalently linked to a lipid moiety termed lipid. Lipid A has been shown to constitute the 'endotoxic principle' of LPS [1,2], although in some biological test systems its activity was found to be significantly lower than that of the parent LPS [3,4]. It was furthermore found that lipid A variants exist which deviate from the common structure of enterobacterial lipid A, a diphosphoryl diglucosamine acetylated with up to seven hydroxylated fatty acid residues in ester or amide linkage. These lipid A variants are found, for example, in *Rhodobacter capsulatus* with only 5 acyl chains (and a length, on the average, of only C-12) and exhibit no biological activity despite identical backbone [5]. These observations provoked the discussion of requirements for

---

* Corresponding author. Fax: +49-4537-188632.

the chemical structure to be fulfilled to induce endotoxicity. It was found that the minimal structure of lipid A expressing biological activity is a backbone composed of two hexosamine saccharides, which are substituted by two phosphates and six fatty acids with defined chain length (not too short and not too long, preferentially C-14, [2,6]) as present in lipid A from *E. coli*. For a detailed study of the dependences of biological activity on chemical structure of lipid A-like samples, previously various synthetic lipid A analogues and partial structures had been synthesized [7,8]. These compounds exhibited pattern of different biological activities ranging from high endotoxicity like interleukin induction in macrophages for compound '506', counterpart of the natural hexaacyl lipid A from *E. coli*, to complete inactivity for compound '406', at least in human-derived macrophages, the latter compound corresponding to the tetraacylated lipid A precursor Ia or IVa [9–13].

It may be obvious that the physical-chemical characteristics of lipid A samples differing in their primary chemical structure, i.e., mainly in the acylation patterns are different in aqueous suspensions. This refers to physical parameters like critical aggregate concentration (CAC, also called critical micellar concentration CMC which, however, may be misleading as not necessarily micellar structures are formed above the CAC), the $\beta \Leftrightarrow \alpha$ gel to liquid crystalline phase transition with transition temperature T_c, and the form and shape of supramolecular aggregates (three-dimensional supramolecular structure, [14–16]). Furthermore, also conformations of the various functional groups like ester and phosphate should be influenced by changes in the chemical structure. Moreover, these physical parameters are, of course, interdependent. For example, an increase in the volume of the hydrophobic moiety by addition of an acyl chain will lead to a reduction of the CAC, to an increase of T_c, and to a stronger tendency to assume nonlamellar inverted structures. Concomitantly, intra- and intermolecular conformations should vary due to changing abilities for hydrogen bonding.
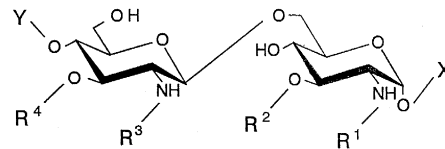
The aims of the present study were the determination of the $\beta \Leftrightarrow \alpha$ gel to liquid crystalline phase behaviour of the hydrocarbon chains, an approximation of the supramolecular aggregate structures and changes between them, and the determination of the intramolecular, within the single molecules, and in-

termolecular conformations, the relative orientation of neighbouring molecules within the aggregates, of synthetic lipid A analogues and partial structures at 37°C. The measurements were performed with Fourier-transform infrared (FTIR) spectroscopy at high water content to guarantee near physiological conditions. The phase behaviour was elucidated by evaluating the symmetric stretching vibration of the methylene groups. For the determination of the supramolecular structure, small-angle X-ray diffraction was performed with natural lipid A from *E. coli* as 'standard'. As for the latter technique high amounts (20 to 30 mg) are needed, an attempt was made to determine the three-dimensional supramolecular structures and changes between them with IR spectroscopy, which affords only minor amounts (< 1 mg) of the samples. This was performed by analysing infrared bands in particular from the interface region, which were shown previously to react sensitively to transitions between, for example, lamellar (L) to nonlamellar cubic (Q) or cubic to inverted hexagonal (H_{II}) structures found in preparations of deep rough mutant LPS or lipid A from *Salmonella minnesota* [17,18]. In this way and also including theoretical calculations on the molecular geometry on the basis of the theory of Israelachvili and co-workers [19,20], an approximation of the structural preferences of the different synthetic lipid A partial structures was possible. A determination of their aggregate structures should be of importance because it was found that the preference to adopt, at least partially, nonlamellar inverted structures is connected directly with the ability of these molecules to express biological activity [16,21–23]. Finally, a detailed study of various IR-active vibrational bands from the polar region like phosphate and ester was performed at 37°C to get closer informations on intra- and intermolecular interactions. This allows, together with the data from the three-dimensional supramolecular structures, to examine possible molecular prerequisites for endotoxic activity.

2. Materials and methods

2.1. Lipid A samples and synthetic structures

In Fig. 1, the chemical structures of the synthetic lipid A analogues and partial structures are given.

| Sample | Substituents | | | | | |
	R^1	R^2	R^3	R^4	X	Y
516	C_{14}-O-C_{16}	C_{14}-OH	C_{14}-O-C_{12}	C_{14}-O-C_{14}	P	P
514	C_{14}-O-C_{16}	C_{14}-OH	C_{14}-O-C_{12}	C_{14}-O-C_{14}	H	P
506	C_{14}-OH	C_{14}-OH	C_{14}-O-C_{12}	C_{14}-O-C_{14}	P	P
505	C_{14}-OH	C_{14}-OH	C_{14}-O-C_{12}	C_{14}-O-C_{14}	P	H
504	C_{14}-OH	C_{14}-OH	C_{14}-O-C_{12}	C_{14}-O-C_{14}	H	P
LA20-PP	C_{14}-O-C_{16}	C_{14}-OH	C_{14}-OH	C_{14}-OH	P	P
LA21-PP	C_{14}-OH	C_{14}-OH	C_{14}-O-C_{16}	C_{14}-OH	P	P
406	C_{14}-OH	C_{14}-OH	C_{14}-OH	C_{14}-OH	P	P
606	C_{14}-OH	H	C_{14}-OH	H	P	P
LA18-PP	C_{14}-OH	C_{14}	C_{14}-OH	C_{14}	P	P
LA17-PP	C_{14}	C_{14}	C_{14}	C_{14}	P	P

Fig. 1. Chemical structures of lipid A analogues and partial structures. Explanation: C_{14}–OH, (R)-3-hydroxy-tetradecanoyl; C_{14}–O–C_{12}, (R)-3-(dodecanoyloxy)-tetradecanoyl; C_{14}–O–C_{14}, (R)-3-(tetradecanoyloxy)-tetradecanoyl; C_{14}–O–C_{16}, (R)-3-(hexadecanoyloxy)-tetradecanoyl; P, phosphates ($H_3PO_4^-$).

They were synthesized as described previously [7,24–26] and are present in the triethylamine (Ten) salt form. Natural lipid A was isolated from LPS of the deep rough mutant strain F515 of *E. coli* by acetate buffer treatment, purified, and converted to the Ten salt form. It differs from compound '506' only by the presence of nonstoichiometric substituents in minor amounts. Triacylated natural lipid A was a kind gift of U. Zähringer (Div. of Immunochemistry, Forschungszentrum Borstel). It is substituted by C_{14}–O–C_{12} in R^3 and by C_{14}–OH in R^1 position.

2.2. Sample preparation

All lipid samples were prepared as aqueous suspensions at high water content, i.e., 96% water content corresponding to ca. 20 mM lipid concentrations in the case of the infrared measurements, and 80% water content in the case of the X-ray diffraction experiments. For some synthetic products, the samples were prepared also at a lower water content (75% corresponding to ca. 170 mM lipid concentration in the case of the hexaacyl lipid A). In all experiments, the lipids were suspended directly in HEPES buffer and were temperature-cycled at least twice between 4 and 70°C and then stored at 4°C at least 12 h before measurement.

The synthetic phospholipid dipalmitoyl phosphatidylcholine (DPPC), used as reference lipid, was purchased from Avanti Polar Lipids (Birmingham, AL).

2.3. FTIR spectroscopy

The infrared spectroscopic measurements were performed on a FTIR spectrometer '5-DX' (Nicolet Instruments, Madison, WI). The lipid samples were placed in a CaF_2 cuvette separated by a 12.5 μm thick teflon spacer. Temperature-scans were performed automatically in the range from 10 to 65–80°C with a heating rate of 3°C/5 min. Every 3°C, 50 interferograms were accumulated, apodized, Fourier transformed, and converted to absorbance spectra.

For strong absorption bands, the evaluation of the band parameters (peak position, band width, and intensity) was performed with the original spectra, if necessary after subtraction of the strong water bands.

Thus, the position of the peak maxima could be determined with a precision of better than 0.1 cm^{-1}. In the case of weak absorption bands, resolution enhancement techniques like Fourier self-deconvolution [27] were applied after base line subtraction. The choice of the three parameters bandwidth, resolution enhancement factor and Gauss/Lorentz ratio important in this procedure was done as described recently [18]. In the case of overlapping bands, in particular for the analysis of the ester carbonyl ν(C=O) and phosphate vibration $\nu_{as}(PO_2^-)$, curve fitting was applied using a modified version of the CURFIT procedure written by Moffat (NRC, Ottawa). An estimation of the number of band components was obtained from deconvolution of the spectra, and the curve fit was then applied within the original spectra after subtraction of base lines resulting from neighbouring bands. Similar to the deconvolution technique, the bandshapes of the single components are superpositions of Gaussian and Lorentzian bandshapes. Best fits were obtained by assuming a Gauss fraction of 0.55–0.60.

The $\beta \Leftrightarrow \alpha$ phase behaviour was monitored by using the peak position of the symmetric stretching vibration $\nu_s(CH_2)$. The phase transition temperature T_c can be determined by taking the midpoint of the intersection of the tangents in the gel phase with that of the inflection point of the transition range, and the intersection of the latter with the tangent in the liquid crystalline phase.

2.4. Small-angle X-ray diffraction

Small-angle X-ray diffraction measurements of natural *E. coli*-lipid A were kindly performed by M.H.J. Koch at the European Molecular Biology Laboratory outstation at the synchrotron radiation facility HASYLAB (c/o DESY, Hamburg) using the double focusing monochromator-mirror camera X33 [28]. Diffraction patterns in the range of the scattering vector $0.07 < s < 1$ nm^{-1} ($s = 2\sin\Theta/n\lambda$, $2\Theta =$ scattering angle, $\lambda =$ wavelength $= 0.15$ nm) were recorded with an exposure time of 2 min using a linear detector with delay line readout [29]. The wavelength calibration was done with tripalmitin having a periodicity of 4.06 nm at room temperature.

The measurements were performed between 20 and 80°C in intervals of 10°C. In the diffraction patterns presented here, the logarithm of the diffraction intensity log I is plotted vs. s, and the evaluation of the X-ray diffraction patterns was achieved according to procedures described previously [14,15].

2.5. Calculation of the critical packing parameter

According to the theory of Israelachvili and co-workers [19,20], the supramolecular structure of lipid aggregates obtained by packing of a large number of single molecules can be approximated by simple geometric parameters like the cross-sections of the hydrophilic and hydrophobic moieties. Thus, only the optimal surface area per molecule a_0 of the polar headgroup, the critical chain length l_c of the hydrocarbon chains which is slightly smaller than the extended chain length, and the volume v of the hydrophobic moiety should be known. The values of l_c and v can be estimated from equations given by Tanford [30] to

$$v = (0.0274 + 0.0269n) \text{ nm}^3 \text{ and}$$

$$l_c = (0.154 + 0.1265n) \text{ nm}$$

per saturated hydrocarbon chain with n carbon atoms. From a knowledge of l_c, v, and a_0 the 'critical packing parameter' $\xi = v/(a_0 l_c)$ can be calculated, which is a determinant for the aggregate structure adopted by the lipids. At $\xi \leq 1/2$, spherical micelles or cylindrical micellar structures like H$_I$, in the range $1/2 \leq \xi \leq 1$ flexible or planar bilayers (lamellar structures), and at $\xi > 1$ inverted structures of cubic symmetry or the inverted hexagonal (H$_{II}$) structure are formed. The most uncertain parameter in the above estimations is a_0, as its value may strongly depend on ambient conditions like temperature and hydration of the headgroup, and, in particular for negatively charged lipids, on the kind and concentration of counterions necessary for compensation of negative charges. Therefore, a reliable prediction of the supramolecular aggregation is only possible if experimental results of reference substances for an approximation of a_0 are available.

3. Results

Three different vibrational bands were analyzed in detail:
(i) the symmetric stretching vibration $\nu_s(CH_2)$ be-
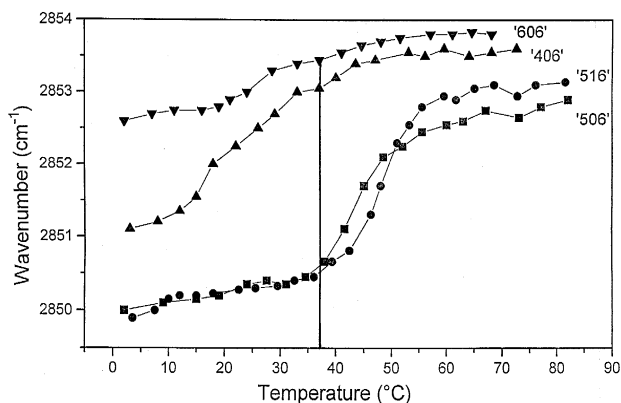
Fig. 2. Peak position of the symmetric stretching vibration $\nu_s(CH_2)$ in dependence on temperature for synthetic bisphosphoryl lipid A analogues and partial structures with two ('606'), four ('406'), six ('506'), and seven ('516') acyl chains.

tween 2880 and 2820 cm^{-1} for the determination of the $\beta \Leftrightarrow \alpha$ phase transition, (ii) the ester carbonyl stretching vibration $\nu(C=O)$ between 1760 and 1700 cm^{-1} as indicator for changes in supramolecular aggregate structure and intra- and intermolecular conformations, and (iii) the antisymmetric stretching vibration of the negatively charged phosphates $\nu_{as}(PO_2^-)$ between 1300 and 1180 cm^{-1} for intra- and intermolecular conformations.

3.1. $\beta \Leftrightarrow \alpha$ phase transition

The peak position of the $\nu_s(CH_2)$-vibrational band, known to be a sensitive marker of lipid order [31],

was evaluated for the different compounds. In Fig. 2, results are presented for some compounds with identical backbone, but different acylation patterns, namely '606' with two, '406' with four, '506' with six, and '516' with seven acyl chains (compare Fig. 1). Clearly, the temperature T_c of the phase transition increases with increasing number of hydrocarbon chains. As was found previously, the wavenumber values should lie around 2850 cm^{-1} in the gel phase and around 2852 to 2853 cm^{-1} in the liquid crystalline phase, it can be deduced that compound '606' is not at all, and '406' only partially in the gel phase in the observed temperature range. Therefore, T_c can only be roughly approximated for compounds '606' and '406' lying below 0°C for the former and around 15 to 20°C for the latter. In Fig. 3, T_c is plotted vs. the number of the acyl chains for the different lipid structures. Also included is the T_c-value for a natural triacylated lipid A partial structure. Obviously, a nearly linear relationship exists between the value of T_c and the number of acyl chains for the samples with hydroxy fatty acids, i.e., '606', triacyl lipid A, '406', LA21-PP, '506', and '516'. The T_c of LA20-PP, carrying three acyl chains at the reducing and two at the nonreducing glucosamine, deviates from this linearity. The observation of linearity implies that the hydrocarbon chain packing density of all samples are similar. Therefore, deviation from linearity to higher T_c-values (LA20-PP) indicates an increase in packing density. It becomes furthermore obvious in Fig. 3 that the number of hydroxy groups in the hydrophobic

Table 1
Phase transition temperature T_c for all investigated lipid A analogues and partial structures

| Sample	No. of acyl chains	T_c (°C)	Remark
606	2	< 0	At 0°C highly fluid
LA-17-PP	4	39	No 3-OH groups
LA-18-PP	4	30	Two 3-OH-groups
406	4	20	Lipid A precursor IVa, 4 OH-groups, transition very broad
LA-20-PP	5	50	Precursor Ib, 3 acyl chains at the reducing, 2 at the nonreducing glucosamine
LA-21-PP	5	31	Two acyl chains at the reducing, 3 at the nonreducing glucosamine
503	6	75	Dephosphoryl lipid A-analogue
504	6	43	Monophosphoryl lipid A-analogue
505	6	48	
506	6	43	Bisphosphoryl analogue of *E. coli*-lipid A
514	7	(38)	Weakly expressed, further transition at 58°C
516	7	48	Analogue of heptaacyl fraction of *S. minnesota*-lipid A
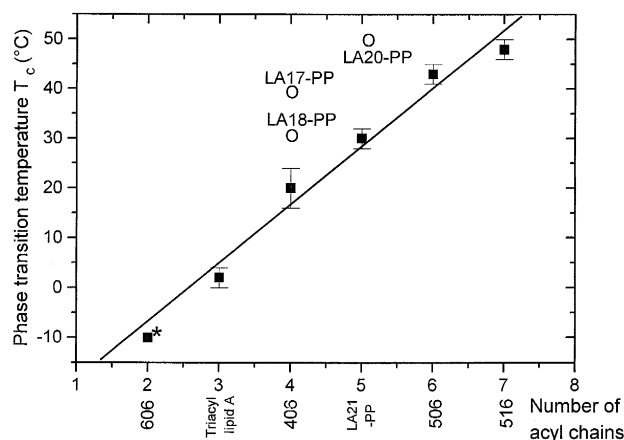
Fig. 3. $\beta \Leftrightarrow \alpha$ phase transition temperature T_c for various synthetic lipid A analogues and partial structures and a natural triacyl lipid A in dependence on the number of acyl chains. Solid line: Regression line obtained for the samples listed below the x-axis. The error bars result from the uncertainty to determine the inflection points of the curves in Fig. 2. For '606' (*), T_c was obtained from an extrapolation.

moiety influences T_c. The removal of two (LA18-PP) or even four (LA17-PP) hydroxy groups leads to a considerable increase of T_c, due to the increase in hydrophobicity.

The data for T_c are summarized in Table 1 for all compounds investigated. Also included is the synthetic compound '503' lacking the two phosphate groups at positions X and Y in Fig. 1. '503' exhibits in the gel phase a relatively high conformational disorder indicated by the peak position of $\nu_s(CH_2)$ lying at 2851.2 cm^{-1}. Interestingly, the T_c-value of the synthetic monophosphoryl lipid A counterpart '504' bearing the 4′-phosphate is the same as that of the synthetic bisphosphoryl sample '506', whereas the synthetic monophosphoryl compound bearing the 1-phosphate, '505', has a significantly higher T_c.

From the peak position of $\nu_s(CH_2)$ at 37°C (see vertical line in Fig. 2) the state of order of the acyl chains for the different compounds can be estimated to be very low (high 'fluidity') for the diacyl and tetraacyl compounds '606' and '406', respectively, and very high for the hexaacyl and heptaacyl products. The two other tetraacyl compounds have, as compared to '406', increasing chain order in the sequence LA18-PP (two hydroxy groups) and LA17-PP (no hydroxy groups). Interesting is also the different acyl chain packing of compounds LA20-PP and

LA21-PP, being high for the former (3/2 configuration of the acyl chains) and medium for the latter (2/3 configuration).

3.2. Three-dimensional structure

For the determination of the three-dimensional organization of lipid aggregates in aqueous suspensions, small-angle X-ray diffraction is usually the method of choice. However, even when synchrotron radiation with its extremely high brilliance is used, still 20 to 30 mg of lipid are necessary as a minimum for a reliable determination of the supramolecular structure under near physiological conditions ($\geq 80\%$ water content). These large amounts are very often not available. To overcome these limitations, another approach was chosen.

(i) By applying synchrotron radiation X-ray diffraction, the supramolecular structures, which for endotoxins comprise lamellar (L), cubic (Q), and inverted hexagonal (H$_{II}$), and the transitions between them were determined under near physiological conditions in the temperature range 20 to 80°C for hexaacyl lipid A from *E. coli*.

(ii) The same lipid A batch measured with X-ray diffraction was analyzed in parallel by IR-spectroscopy and then used as a 'calibration standard' to assign particular characteristics of band contours and their changes to supramolecular structures and to structural transitions.

This is readily feasible since structural transitions like L $\Leftrightarrow$ H$_{II}$ or cubic Q $\Leftrightarrow$ H$_{II}$ are accompanied by characteristic changes of IR-active band contours in the interface region like ester and amide, as was recently found for LPS Re from *S. minnesota* R595 [18]. In particular, the most pronounced changes of, e.g., bandwidth and peak position, can be observed at the transition into H$_{II}$, either from a cubic or a lamellar structure. Moreover, the peak position of some band components can be characteristic for a particular supramolecular structure, e.g., in the case of the H$_{II}$ structure.

(iii) The behaviour of natural lipid A was then compared with that of the synthetic counterpart, the hexaacyl lipid A analogue '506'. This is a reasonable approach, because the main component of lipid A from *E. coli* is a hexaacyl lipid A (content $\geq 80\%$)
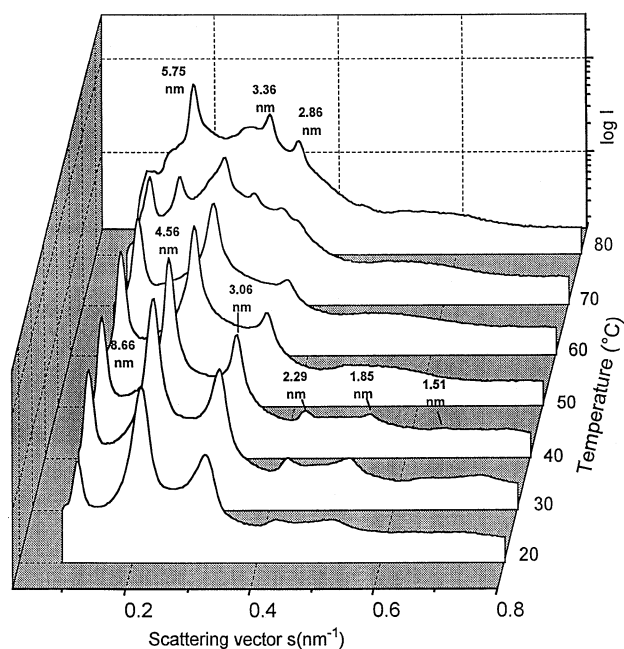
Fig. 4. Small-angle X-ray diffraction patterns for lipid A from *E. coli* LPS F515 at 80% water content and [lipid A]:[Mg^{2+}] 10:1 M in the temperature range 20 to 80°C. For the diffraction patterns at 40 and 80°C, the spacing ratios of the reflections $d = 1/s$ are given.

identical to '506'. From this comparison, it should then be possible to obtain data on the structural preferences of this synthetic compound only from infrared data.

(iv) From the results for compound '506', also an approximation of the supramolecular structures of the other synthetic lipid A analogues and part structures like heptaacyl lipid A '516' can be obtained on the basis of the theory of Israelachvili [19,20]. The results for the former compound should give a reasonable estimate of the optimal surface area/molecule a_o, which should, in first approximation, be similar for all synthetic products with identical backbone. Therefore, for the bisphosphoryl compounds the critical packing parameter can be calculated and, with that, an estimate of their structural preferences.

Small-angle diffraction patterns for lipid A are presented in Fig. 4 in the temperature range 20 to 80°C at 80% water content. A detailed analysis (for a nearer description of the methodology see former publications [14,21,33,34]) shows the occurrence of mixed cubic (Q$_1$)/lamellar (L) structures in the range 20 to 50°C, a pure cubic (Q$_2$) structure between 50 and 70°C, and the H$_{II}$ structure above 70°C. For
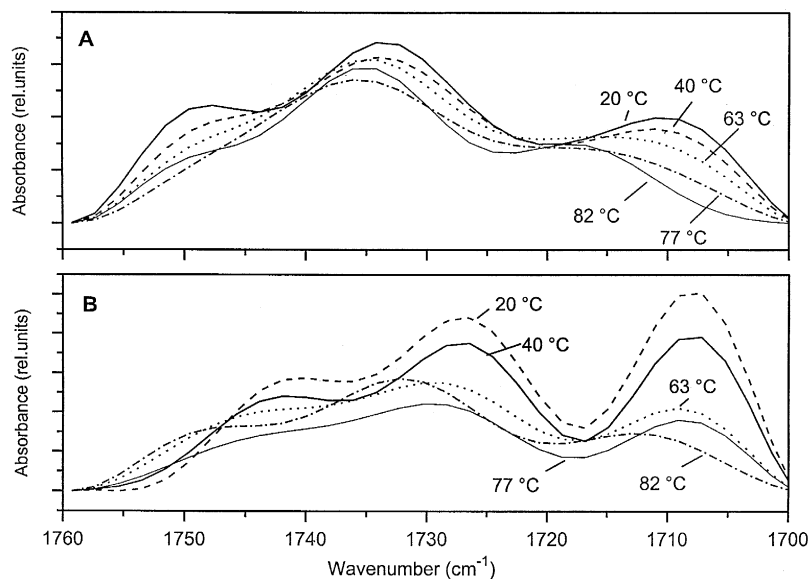

Fig. 5. Deconvoluted spectra in the range of the ester carbonyl stretch ν(C=O) for lipid A from *E. coli* LPS F515 (A) and synthetic hexaacyl lipid A '506' (B) at various temperatures and at a water content of 75%. Deconvolution parameters: 26/1.6 (bandwidth/resolution enhancement factor).

example, at 40°C reflections are found at 8.66, 4.56, 3.06, 2.29, 1.85, and 1.51 nm, which can be grouped into 3.06 nm $= d_Q/\sqrt{8}$, 2.29 nm $= d_Q/\sqrt{14}$, 1.85 nm $= d_Q/\sqrt{22}$, and 1.51 nm $= d_Q/\sqrt{32}$, with $d_Q \approx 8.70$ nm as cubic periodicity and a remaining lamellar structure with $d_1 = 4.56$ nm. The intermediate cubic structure Q_2 is not resolvable in a straightforward way. At 80°C, the reflections at $d_H = 5.75$ nm and 3.36 nm $= d_H/\sqrt{3}$ and 2.86 nm $= d_H/\sqrt{4}$ prove the existence of the H_{II} structure. Therefore, from these measurements a thermotropism $Q_1/L \Leftrightarrow Q_2 \Leftrightarrow H_{II}$ can be derived, and the former transition seems to be roughly connected with the $\beta \Leftrightarrow \alpha$ chain melting process.

The IR-analysis was performed by procedures described earlier [18], and comprises the temperature dependences of the band position and bandwidth of deconvoluted spectra from the ester and amide groups, in particular their low frequency components, which were shown to respond sensitively to changes in supramolecular organization. As an example, the ester band contours (deconvoluted spectra) are plotted for lipid A from *E. coli* (Fig. 5A) as well as for its synthetic analogue '506' (Fig. 5B) at some selected temperatures showing drastic changes in particular of the low frequency band at 1710 cm^{-1}. A detailed analysis of the temperature dependence of this band is given in Fig. 6 for lipid A (A) and is compared with the respective behaviour of the synthetic samples '506' and '516' (B). For the natural lipid A, the transition into H_{II} around 75°C is clearly expressed as proven by the shift of the band position to higher
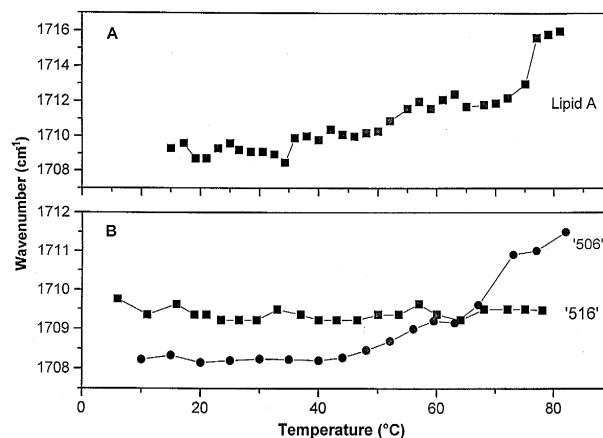

Fig. 6. Peak position of the low frequency band component of the ester carbonyl stretch $\nu(C=O)$ in dependence on temperature for lipid A from *E. coli* LPS F515 (A) and synthetic lipid A analogues hexaacyl '506' and heptaacyl '516' (B). The evaluation was performed with deconvoluted spectra as given in Fig. 5.

wavenumbers. Similarly, the $Q_1/L \Leftrightarrow Q_2$ transition at 50 to 55°C becomes apparent by an increase in band position analogously to the behaviour previously shown for the $Q_1 \Leftrightarrow Q_2$ transition of LPS Re [18]. Importantly, for '506' the spectral features seem to be very much alike those of lipid A, slight increase of the wavenumber at 50 to 60°C and a stronger one around 70°C. This indicates a similar structural sequence Q_1 (or Q_1/L), Q_2, H_{II} for the synthetic compound. Furthermore, from the absence of any significant change in peak position over the entire temperature range for the heptaacyl lipid A analogue

Table 2

Critical packing parameter ξ and prediction of supramolecular structures deduced from ξ for various synthetic compounds

Compound	No. of acyl chains	Critical packing parameter ξ	Supramolecular structure (prediction)	Remark
'606'	2	0.33	Micellar (M)	
Triacyl lipid A	3	0.49	M or L	Measured: Micellar H_I (unpublished)
LA17-PP	4	0.66	L	
LA18-PP	4	0.66	L	
'406'	4	0.66	L	Measured: L for lipid A from *Rb. capsulatus* [22]
LA20-PP	5	0.83	L	
LA21-PP	5	0.83		
'506'	6	≥ 1.00	Q and/or H_{II}	Measured: Q at 40°C, H_{II} at 70°C for lipid A from *E. coli* [14,18]
'516'	7	1.28	Q/H_{II}	

The measured supramolecular structures in the right column were obtained from some natural isolates with high structural similarity to the respective synthetic products.

'516' the existence of transitions between mixed cubic/lamellar and pure cubic or between pure cubic structures as well as those into the inverted hexagonal phase can be excluded, whereas a natural heptaacyl lipid A isolated from the thermosensitive sscI mutant of *S. thyphimurium* SH7622 [35] exhibits a drastic change of band parameters (position and bandwidth) of the low frequency ester and amide II band components directly above T_c, identical to that of '516' at 48°C (data not shown).

From the application of the theory of Israelachvili a lower limit for the critical packing parameter of $\xi = 1$ (boundary lamellar/inverted) for lipid A and '506' can be assumed. Applying the formula introduced by Tanford for the space requirement of the hydrophobic moiety v and the critical chain length l_c, the optimal area/molecule can be calculated to $a_o = 1.273$ nm^2 assuming that all C14–OH or C14–O–C$_n$ chains have an effective chain length of C12 (this assumption might be justified because of the existence of the 3-OH or 3-O–acyl groups). In Table 2, predictions of the supramolecular structural preferences are given for all compounds with identical (bisphosphoryl diglucosamine) backbones. As $\xi = 1$ for '506' is a lower boundary, the values of a_o might, realistically, be lower and, with that, the structures given in Table 2 might be more inverted as listed in the table. Due to the fact that values of a_0 are not known for the monophosphoryl products '504' and '505', the supramolecular structures of these compounds cannot readily be estimated. However, if it is assumed that the value of a_o is lower than that of '506' because of the smaller backbone and reduced repulsive forces between adjacent phosphate groups, ξ might be estimated to be > 1, i.e., inverted structures should be expected also for the monophosphoryl compounds.

For the triacylated compound we have found a micellar H$_I$ structure (own unpublished results). This result is completely in agreement with the prediction given in Table 2 as H$_I$ structures are expected to appear at the border micellar/lamellar. The predictions for the tetraacyl samples can be related directly to structural determinations of lipid A from *Rhodobacter capsulatus* having a similar volume of its hydrophobic portion and adopting a clear multi-lamellar organization [22]. The synthetic heptaacyl sample should have a clear tendency to adopt an inverted structure, presumably H$_{II}$ at least above the phase transition temperature (48°C), whereas, surprisingly, the IR data presented in Fig. 6 exclude this possibility.

3.3. Intra- and intermolecular conformations at 37°C

Beside the determination of the organization of large numbers of individual molecules within a macroscopic aggregate (supramolecular structure), the analysis of individual functional groups is of fundamental importance for the determination of intra- and intermolecular conformations in particular when regarding experimental findings that endotoxicity could be mainly exerted by monomers or small oligo- or polymers [36,37]. The phosphate groups belong to one of the most important functional groups, especially when considering that the existence of at least one phosphate group was found to be essential for the expression of endotoxic activity [6].

A comprehensive analysis was performed with the antisymmetric stretching vibration of the negatively charged phosphate $\nu_{as}(PO_2^-)$ in the wavenumber range 1300 to 1180 cm^{-1} applying curve fitting procedures as described in Section 2. It should be emphasized, that this vibrational band usually consists of two or more single components, the location and intensity of which are connected with different degrees of hydration [38]. Thus, band components corresponding to undisturbed vibrations can be found in the wavenumber range 1250 to 1265 cm^{-1}, whereas vibrations disturbed by water adsorption give rise to bands between 1230 and 1245 cm^{-1}, and for extremely high hydration at 1200 to 1225 cm^{-1}. In Fig. 7a, the spectral range 1320 to 1180 cm^{-1} is plotted for the synthetic samples with identical acyl moiety but different phosphate substitution. Presented are the single band components obtained by curve fitting, their sum is nearly identical with the original spectrum (envelope curve, thick line). For '506', beside the small band at 1261 cm^{-1}, one strong band at high wavenumbers, one smaller component at medium and one strong and broad band at lower wavenumbers (see also Table 3) are obtained. For the monophosphoryl samples '504' (only 4′-phosphate) and '505' (only 1-phosphate) a complex splitting of the band in single components is observed which cannot readily be assigned to the respective 1- or 4′-phosphate
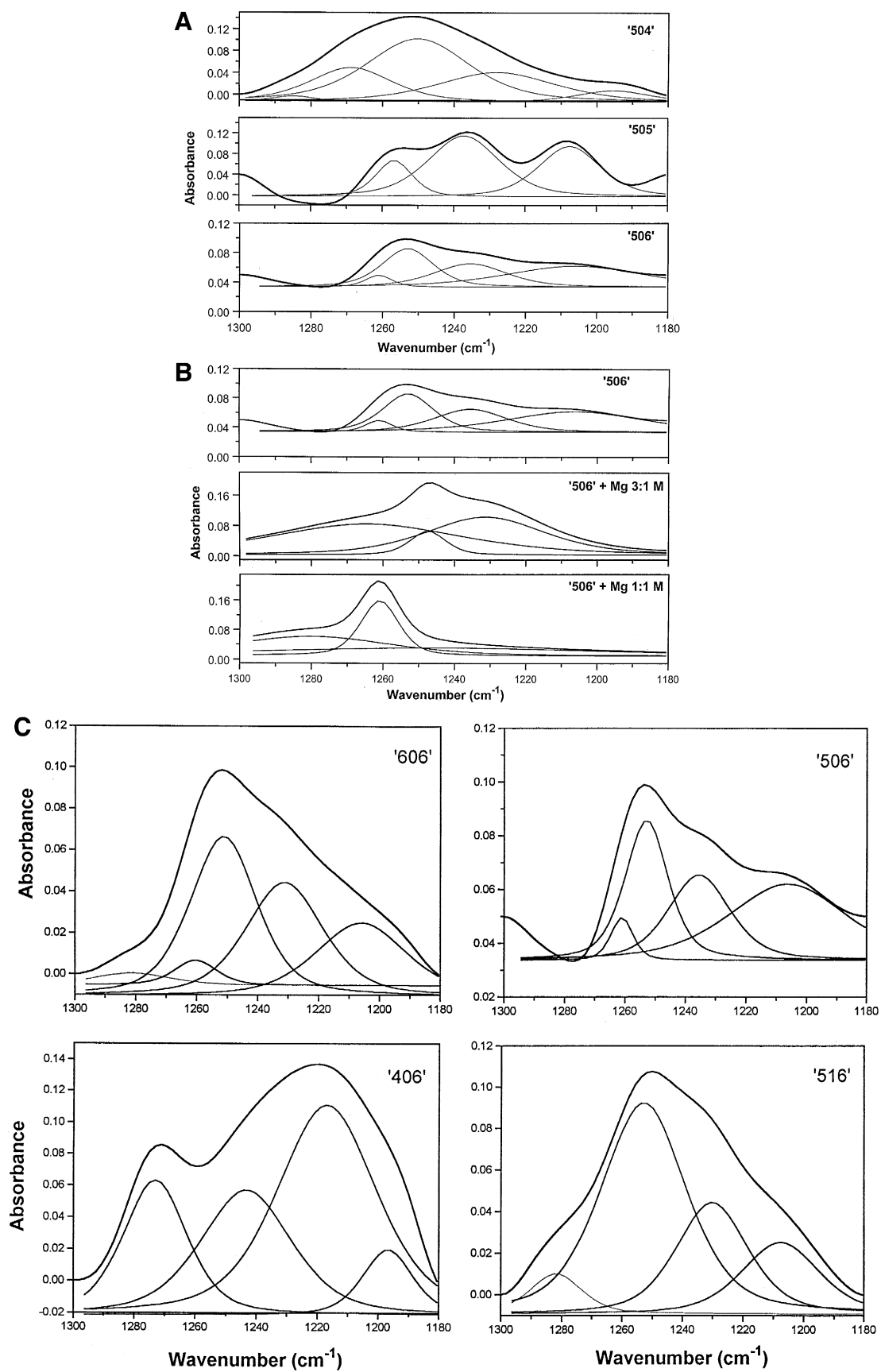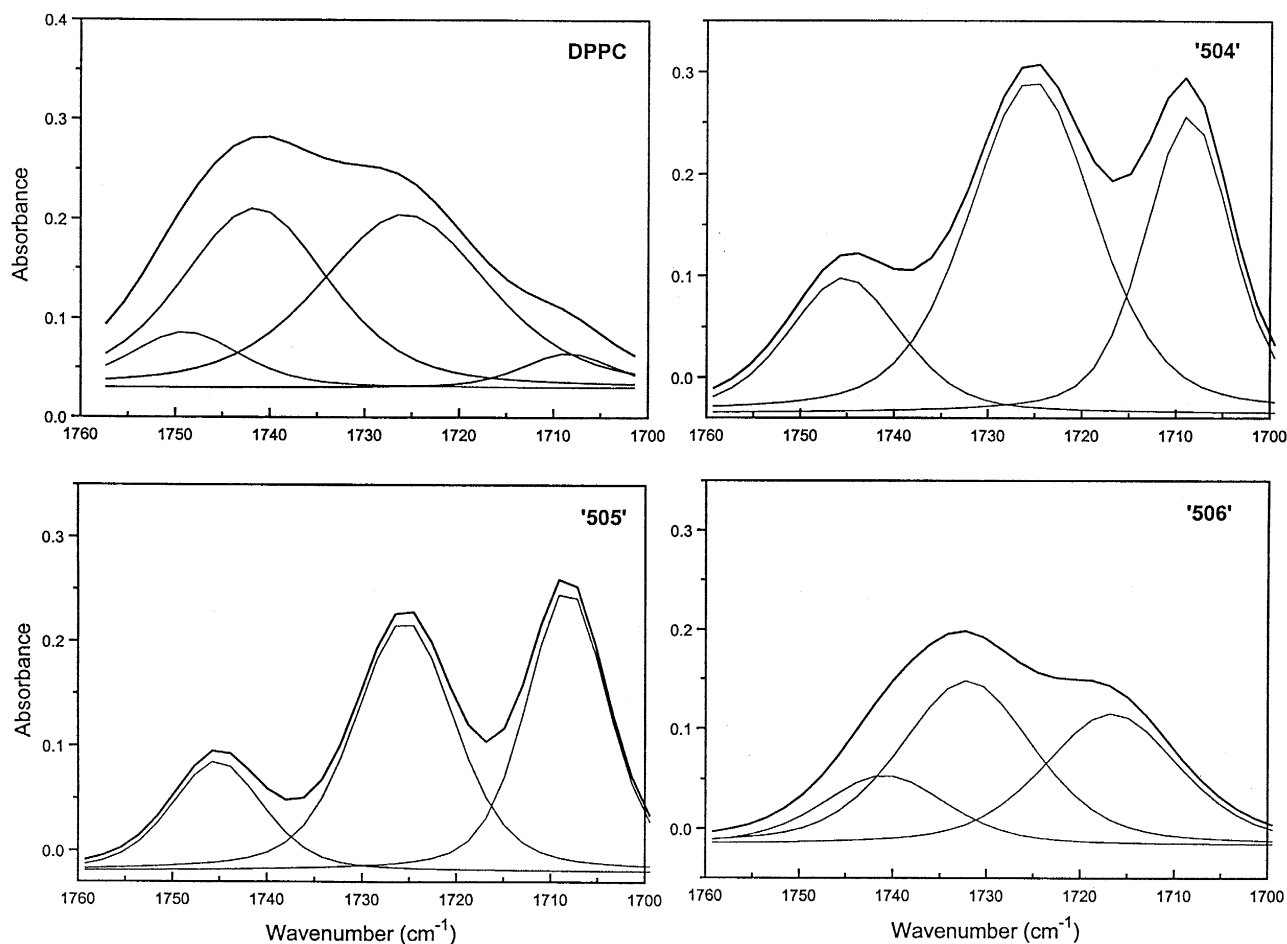
Fig. 8. Spectra in the wavenumber range of the ester carbonyl stretch ν(C=O) and single band components obtained from curve fitting for hexaacyl lipid A analogues '504' (1-phosphoryl), '505' (4′-phosphoryl), and '506' (bisphosphoryl). Spectra were obtained at 37°C and at 75% water content.

groups. Whereas for '505' two dominant components around 1207 and 1237 cm^{-1} and a higher wavenumber component with a much lower intensity were found, the situation for '504' is just the opposite with the two most abundant band components around 1268 and 1250 cm^{-1}. This implies a much stronger hydration of the 1- as compared to the 4′-phosphate. Consequently, in the spectrum of '506', composed of the

contributions of both groups, a superposition of one strongly hydrated state of the 1-phosphate and two further states with medium to low hydration, predominantly caused by the 4′-phosphate are observed. However, the band contour of '506' has a significantly higher overall similarity to '505' than to '504'.

In Fig. 7b, the influence of Mg^{2+} on the hydrational states is presented exemplarily for hexaacyl

Fig. 7. Spectra in the wavenumber range of the antisymmetric stretch of the negatively charged phosphate ν_{as}(PO$_2^-$) and single band components obtained by curve fitting assuming a Gaussian fraction of 0.55 for (A) hexaacyl lipid A analogues '504' (1-phosphoryl), '505' (4′-phosphoryl), and bisphosphoryl '506', (B) hexaacyl bisphosphoryl lipid A at varying Mg^{2+} concentrations, and (C) bisphosphoryl lipid A analogues and partial structures with two ('606'), four ('406'), six ('506'), and seven ('516') acyl chains. Spectra were obtained at 37°C.

Table 3
Single band components of the phosphate vibration $\nu_{as}(PO_2^-)$ with half-value width (full width at half height) and relative intensities obtained from curve fitting of the original spectra

Sample/no. acyl chains	Position/ cm^{-1}	Half-value width/cm^{-1}	Rel. intensity
606	1281.5	29.7	0.17
	1260.5	16.4	0.22
2	1251.4	25.9	1.00
	1231.3	30.3	0.83
	1206.1	30.4	0.56
406	1273.6	24.3	1.03
	1245.6	31.4	1.00
4	1218.8	40.8	2.96
	1198.0	19.9	0.38
LA17-PP	1256.7	25.0	0.52
	1232.9	36.7	1.00
4	1206.6	32.3	0.23
LA18-PP	1253.0	32.4	1.10
	1233.2	32.6	1.00
4	1213.3	17.0	0.08
LA21-PP	1261.5	11.2	0.10
	1254.5	21.6	1.00
5	1235.6	28.1	0.76
	1211.5	40.6	0.93
504	1268.4	20.9	0.49
	1251.9	28.1	1.00
6	1232.3	31.7	0.65
	1200.1	34.8	0.29
505	1256.8	12.9	1.00
6	1237.2	23.4	3.00
	1207.6	21.1	2.34
506	1261.0	8.3	0.20
	1253.1	16.3	1.00
6	1235.9	26.3	1.10
	1205.7	44.2	1.50
506+Mg^{2+}	1264.6	64.1	6.70
3:1 M	1247.4	11.8	1.00
	1231.3	39.7	5.14
506+Mg^{2+}	1280.1	52.2	1.40
1:1 M	1261.0	12.6	1.00
	1245.1	112.6	1.27
514	1256.9	21.8	1.00
7	1241.8	51.1	3.70
	1203.5	39.9	0.70
516	1281.0	21.2	0.31
	1262.1	23.0	0.55
7	1249.9	23.7	1.00
	1232.2	25.8	0.93
	1209.8	32.7	0.76

The intensities are related to the normalized intensities of the band components between 1260 and 1245 cm^{-1}. The precision of the band position can be estimated to be 2 cm^{-1} obtained from variations of the Gauss fraction in the range 0.50 to 0.65.

'506'. At lower Mg^{2+} content, the low-wavenumber band component already disappears, while an extremely broad high-wavenumber component is observed. At higher Mg^{2+} content, only two high-wavenumber components exist indicating a complete Mg^{2+}-induced dehydration of the phosphate groups.

Finally, in Fig. 7c the synthetic samples with identical polar backbone but varying number of acyl chains are compared. Although the locations of the band components of '506' and '516' are similar (neglecting the weak band at 1281 cm^{-1} for '516' which does probably not result from the phosphates), the relative band intensities for the band components around 1250, 1230, and 1208 cm^{-1} are 1:1.1:1.5 for '506' and 1:0.93:0.76 for '516', respectively. This implies that '516' is in a more dehydrated state than '506'. Striking is the observation of the intense band components in the spectrum of '406' indicating extremely high hydration. The headgroup conformation of '406' seems to be changed completely as compared to the other samples. This is valid not only at 37°C, but in the entire temperature range 15 to 50°C. The phosphate group hydration of compound '606', which was shown to adopt a micellar structure (Table 2), is not very pronounced. It is lower than for '506' and seems rather to be similar to that of the heptaacyl '516'. A complete picture of the splitting of the $\nu_{as}(PO_2^-)$ band contour into the single components by curve fitting is given in Table 3. The precision of the band positions of the single components can be estimated to be ca. 2 cm^{-1}, which was deduced from variations of the Gauss/Lorentz ratio in the range 0.50 to 0.65. From a comparison of the tetraacyl compounds '406', LA17-PP, and LA18-PP, again the importance of the 3-OH groups becomes evident. The data indicate an increase of the relative intensity of band components due to lesser hydration (1253 to 1256 cm^{-1}) for the samples with decreasing numbers of OH-groups in the acyl chain region. The comparison of the monophosphoryl compounds '504' and '514' with 6 and 7 acyl chains, respectively, does not provide evidence for strong differences in the hydration conditions but in the splitting of the bands with a more homogeneous phosphate environment of sample '514' which may be connected with a changed three-dimensional structure.

Also, the ester carbonyl stretching band contour

already utilized above for the elucidation of changes in the three-dimensional structure (Fig. 5) was analyzed for the hexaacyl synthetic compounds at constant temperature (37°C) and at a water content of 75%, to avoid the superposition by the strong OH-bending at 1650 cm^{-1}. The results from curve fitting of the original spectra are given in Fig. 8 for the samples '504', '505', and '506' and compared to that of DPPC. It should be noted that the splitting of the ester bands are batch-dependent. For example, the spectrum for the DPPC batch obtained from Avanti Polar Lipids was well-resolved whereas those from batches from other origin were less resolved, the low frequency band exhibiting only a slight shoulder at 1725 to 1730 cm^{-1}.

Clearly, the lipid A analogues exhibit a high intensity frequency band component between 1708 and 1715 cm^{-1}, which is only present with low intensity or not at all for DPPC. The occurrence of the low frequency component can be interpreted to result from strong hydrogen bonding [39] of the synthetic samples which is much lower, but still present (band at 1725 cm^{-1}) for DPPC. It can clearly be taken from Fig. 8 that the number of ester groups (4 in the lipid A analogues, 2 in DPPC) is not responsible for the ester carbonyl band splitting. The spectra of the two monophosphoryl samples are surprisingly well-resolved and very similar, but different from that of '506' clearly demonstrating the influence of phosphate substitution on the hydration of the interface region. In particular, the location as well as the intensity of the low frequency band indicates for '504' and '505' an even stronger hydrogen bonding to the ester groups than for '506'. Furthermore, the addition of Mg^{2+} cations (data not shown) leads to a change of the intensity ratio of the lower to the medium frequency (1725 to 1730 cm^{-1}) in favour of the former which is indicative of an increase of water binding to the ester groups. This effect is only marginal for '506', its low frequency band is a priori relatively strong (Fig. 6b), but clearly expressed for lipid A. Consequently, in the presence of Mg^{2+} the spectra of lipid A and '506' are very similar.

Compound '406' again behaves quite different with respect to the position of the two low frequency components at 1718 and 1738 cm^{-1} indicating different conformations of the two remaining ester groups (not shown).

4. Discussion

4.1. Phase transition temperature T_c

The temperature T_c of the β ⇔ α acyl chain melting transition is for the 3-hydroxylated compounds, except for LA20-PP, nearly linearly dependent on the number of acyl chains (Fig. 3). From this, a similar packing density of their hydrocarbon chains can be deduced considering results found for saturated C-12 to C18 lecithins, which show a nearly linear increase of T_c and ΔH_c with increasing acyl chain length [40]. In a similar way, the increase of the T_c-values for the tetraacyl compounds from '406' (four OH groups) over LA18-PP (two OH-groups) to LA17-PP (no OH-groups) is an expression of the increasing hydrophobicity. Interesting is the higher T_c of the synthetic precursor Ib LA20-PP with 3 acyl chains linked to the reducing and 2 to the nonreducing side of the diglucosamine as compared to that of the isomer LA21-PP with a reversed linkage. This emphasizes the importance of the linkage type and the acylation pattern governing the packing density of the hydrocarbon chains and should be important in the light of known differences of lipid A structures like that of the nonenterobacterial species *Chromobacterium violaceum*. In this lipid A, the acyl chains are linked in a 3/3 configuration to the diglucosamine [11] rather than in a 4/2 configuration as for lipid A from *E. coli* and '506'.

4.2. Supramolecular structure

The characterization of the supramolecular structure of endotoxin aggregates in aqueous dispersions is important for the determination of the molecular shape of the individual molecules which was found to be a determinant of endotoxicity of lipid A [22,32]. The method of choice for the elucidation of the three-dimensional supramolecular structure is small-angle X-ray diffraction. For this, however, also when utilizing synchrotron radiation at least 20 to 30 mg of sample material are required. Therefore, an indirect approach was chosen by determining the aggregate structures in dependence on temperature for the 'calibration standard' natural hexaacyl lipid A with X-ray diffraction (Fig. 4) and correlating particular changes of the ester band contours (Figs. 5 and 6) to

the observed changes of the aggregate structure. The fact that synthetic hexaacyl lipid A '506' exhibits the same characteristic changes of the band contours (Fig. 6) allows an assignment of this compound to an inverted structure (cubic, H_{II}) and, with that, to a minimal value of the packing parameter of $\xi = 1$. From this, a determination of the parameter a_0 is now possible for all synthetic products with the same diphosphorylated backbone and, with that, of their three-dimensional structural preference. The approximation of a_0 does not consider a possible inclination of the diglucosamine backbone with respect to the membrane normal as proposed for the hexaacyl compound (see next paragraph). Assuming an inclination angle of 30°, the decrease in the effective a_0 would lead to an increase in ξ by ca. 15% which, however, would not change the predicted aggregate structures of the tetra- to heptaacyl compounds. Only the triacyl compound would now unequivocally adopt a lamellar structure. For this compound, however, own X-ray diffraction measurements indicate the existence of the H_I structure, preferentially occurring between M and L structures, which is thus in excellent accordance with the structural prediction.

It should be emphasized that detailed statements on the thermotropic phase behaviour of the single synthetic products cannot be given. The results for one single compound, natural lipid A (Fig. 4), clearly demonstrate the complexity of the aggregate structures occurring already at one fixed water content. Therefore, for a knowledge of the detailed structural polymorphism, each synthetic compound must be analyzed separately. However, this was not in the scope of the present paper. Rather, the basic tendency for each compound to assume M, L, or inverted Q, H_{II} structures was the main interest and the results seems to be of fundamental importance with respect to the expression of biological activity (see later paragraph).

Temperature-induced changes in supramolecular structures are accompanied by characteristic changes occurring in band contours of vibrations resulting from the interface region like ester. The fact that the heptaacyl compound '516' does not express such changes, i.e., does not pass into the H_{II} structure (Fig. 6) above T_c is difficult to understand from the value of the critical packing parameter (Table 2) and also in the light of the fact, that the natural heptaacyl

lipid A from *S. thyphimurium* assumes the H_{II} structure above 50 to 55°C. One may speculate that a higher affinity for lamellar structures for '516' as compared to '506' may have a noticeable effect on the biological activity. And in fact, it was shown that '516' is significantly less active than lipid A from *E. coli* or '506' in typical in vivo tests (lethality and pyrogenicity) as well as in vitro systems (antigenicity and macrophage activation [9–12]), whereas the natural heptaacyl lipid A showed similar activity as natural hexaacyl lipid A (A. Schromm, private communication). However, the lack of one of the two 3-OH groups, the lower CAC, and the lower 'solubility' in water for compound '516' as compared to the hexaacyl samples may also modify the biological activity.

4.3. Intra- and intermolecular conformations

The analysis of the vibrational bands of the phosphates makes obvious considerable differences between the bisphosphoryl compounds (Fig. 7c). This clearly emphasizes the importance of variations of the acyl chain structure for the expression of various different complex hydrational states of the two phosphate groups. In particular, '406' exhibits the highest degree of hydration. This might be correlated with the lamellar supramolecular structure of compound '406' and, probably, the absence of any inclination of its acyl chains with respect to the membrane normal allowing a good access of water molecules to the phosphate groups. Such access might be hampered for the compounds '506' and '516' assuming inverted structures and, possibly, also an inclination of the acyl chains with respect to the membrane normal (see model below). However, the comparison with the hydration states of '606' with its micellar structure, also allowing access of water to the phosphates, indicates also other influences. For example, the high amount of OH-groups in '406' might be important. These strictly hydrophilic groups close to the backbone may lead to the formation of an ordered water layer along the whole interface region including not only the phosphate groups intra- but also intermolecularly.

The results obtained from these conformational studies, from data of the phase transition behaviour and from former investigations [41,42] now allow to give a schematic diagram of the packing of neigh-
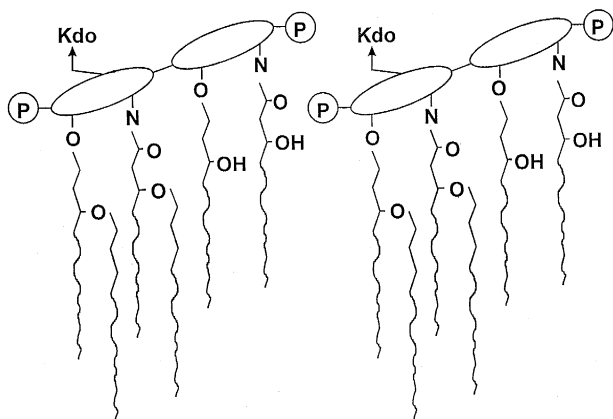
Fig. 9. Model of the intermolecular conformation of neighbouring LPS molecules; Kdo = 2-*keto*-3-deoxyoctonate (further explanation see text).

bouring lipid A molecules (Fig. 9). The lipid A diglucosamine backbone is oriented at an angle of 20 to 40° with respect to the membrane normal with the 1-phosphate surrounded by a pure aqueous environment, whereas the 4′-phosphate is buried in the backbone-close hydrophobic region probably facing the 3-hydroxy groups of the neighbouring molecule. The existence of this particular intermolecular conformation is a new finding but is backed by several observations and considerations: (i) The results from the phosphate band analysis indicate a highly hydrated 1- and a much less hydrated 4′-phosphate, and the former state was strongest expressed in '506' (Fig. 7a). (ii) Results from IR ATR measurements gave dichroitic ratios of 1.10 to 1.25 for a sugar band at 1075 cm^{-1}, which indicates an inclination of the diglucosamine backbone as described above [41].

Computer model calculations also yielded a similar inclination leading to a hexagonal dense packing of the acyl chains similar as found for phospholipids [43,44]. However, from the model calculations using energy minimization techniques a reversed inclination was postulated, i.e., the 1-phosphate buried in the hydrophobic part of the neighbouring molecules and the 4′-phosphate directed towards the water phase. Assuming an intermolecular conformation as proposed here (Fig. 9), the computer calculations led to a much more unfavourable packing of the acyl chains being far away from a close packing [45]. However, our model nevertheless seems to be realistic in the light of two further observations

(i) Some of the synthetic compounds, i.e., LA17-PP, LA18-PP, and LA20-PP (Fig. 3) melt at a considerably higher T_c. From this, it may be deduced that they have a significant closer packing of their hydrocarbon chains than the respective isomers, in particular than the other synthetic products like '506' which, again, cannot be closely packed.

(ii) In calorimetric measurements it was found that the enthalpies of the β ⇔ α acyl chain melting transition for LPS R-mutants lies around 30 to 33 kJ mol^{-1} (for lipid A even around 15 to 25 kJ mol^{-1}), and is with that much lower than for saturated phospholipids like DMPC and DMPE, if taken on the basis of the total number of methylene groups [42]. Even if the effective length of the hydrocarbon chains was assumed to be only C-12 due to the presence of the OH-groups, the resulting 72 C-atoms should yield ΔH-values around 72 kJ mol^{-1}. This again indicates that the samples in Fig. 3 obeying the linear dependence of T_c versus acyl chain number are, due to the existence of the 3-OH and 3-O–acyl groups, not closely packed.

Furthermore, it should be considered that the computer calculations were performed for single molecules in vacuo, i.e., neglecting the influence of water and neighbouring molecules and may, therefore, lead to wrong conclusions.

Our findings are in good agreement with the early findings of Emmerling and co-workers [46] who stated that ''the ordered state of the hydrocarbon chains was less well developed than in most biological membranes and lipids''. Instead of the 0.42 nm X-ray wide angle reflection attributable to the β-type ordered conformation of the hydrocarbon chains (gel phase), they found for hydrated *E. coli* wild-type LPS one reflection at 0.433 nm which converted to a diffuse reflection at 0.45 nm at 35°C typical for the α-phase. In contrast, Labischinski et al. [44] found a wide-angle reflection at 0.425 nm for dried samples of lipid A, LPS Re, and LPS *S*-form which, however, remained unchanged up to 50°C. Thus, these results clearly indicate that the dried endotoxin samples allow a much higher packing density of the acyl chains and, concomitantly, do not even undergo the β ⇔ α transition. These results were confirmed by later investigations into the structural polymorphism of lipid A and rough mutant LPS from *S. minnesota*, in which highly ordered multilamellar stacks were found

at lower water content ($\leq 50\%$) and increasingly unilamellar or nonlamellar structures at higher water content [33,34].

4.4. Influence of Mg^{2+}

Divalent cations like Mg^{2+} and Ca^{2+} are known to be essential not only for the stability of the outer membrane of the bacteria but also for the expression of biological activity of endotoxin [46]. Furthermore, it was shown previously that addition of Mg^{2+} at molar concentrations of [endotoxin]:$[Mg^{2+}] \leq 1$ led to (a) an increase of the T_c values and of the states of order in both phases and (b) to a transition into a multibilayered organization from a nonlamellar or mixed lamellar/nonlamellar (lipid A, short sugar-chain LPS, i.e., mutants Re and Rd) or unilamellar structure (longer sugar-chain LPS, i.e., Rc to Ra) [16,21].

From the evaluation of intra- and intermolecular conformations, performed exemplarily for '506', drastic effects of Mg^{2+} on hydration states could be deduced. Thus, for example, a decrease in hydration was observed for the phosphate groups but an increase for the ester groups (Fig. 7b). The decrease can be explained by a direct binding of Mg^{2+} cations to the negatively charged phosphate groups leading to a loss of bound water, whereas the increase of hydration of the ester groups should be due to a more indirect action of Mg^{2+} cations which are known to form a hydration shell. These 'hydrated cations' may interact predominantly with uncharged but polar groups of the interface region thus stabilizing the intra- and intermolecular order leading, together with the Mg^{2+} bound to the phosphate, to an increase of multilamellar structures.

4.5. Comparison with literature data

Although various investigations into the elucidation of the $\beta \Leftrightarrow \alpha$ acyl chain behaviour and the supramolecular arrangement of natural lipid A and LPS preparations (see [14,33,42,43,46]) have been performed, very few data are available regarding biophysical studies on chemically well defined synthetic lipid A and part structures. Thus, Naumann et al. [48] found T_c-values of 44 and 47°C for compounds '506' and '516', respectively, being in accor-

dance to our data. Labischinski et al. [49] reported on conformational studies of bacterial and synthetic lipid A partial structures comprising also the products '406', '506', and '516'. These authors concluded in accordance with our findings that the synthetic heptaacyl compound '516' revealed an unexpected conformational behaviour with a different acyl chain packing than the other synthetic compounds and that the ester carbonyl groups of '506' and '516' are involved in much stronger hydrogen bonding as compared to phospholipids like DPPC.

4.6. Correlation to biological activity

It was found previously that a peculiar conformation of lipid A is a prerequisite for the expression of endotoxicity [1,4,47]. We have found that this conformation should comprise a higher cross-section of the hydrophobic as compared to the hydrophilic moiety, i.e., a conical shape of the lipid A molecule leading to nonlamellar inverted supramolecular structures of the lipid A aggregates as observed in Fig. 4 [23,32]. The dependence of the peak position of the ester band component (Fig. 6) on temperature for '506', which is identical to that of lipid A, now allows the assignment of the aggregate structure also of this compound to a mixed cubic/lamellar or pure cubic at $T \leq 55°C$, a second cubic at $55°C \leq T \leq 70°C$, and the H_{II} phase at $T \geq 70°C$. Furthermore, a definition of the parameter a_o and with that, a structural prediction for the various bisphosphoryl products with two ('606'), four ('406', LA17-PP, LA18-PP), and five acyl chains (LA20-PP, LA21-PP) is now possible (see Table 3). For all these compounds, no biological activity has been reported [12,50,51] at least with respect to cytokine production in human monocytes/macrophages. This should be due to the missing ability of these products to adopt conical-shaped conformations of the individual constituting molecules as described above.

The structural preference of monophosphoryl lipid A samples could recently be determined for hexaacyl, but also pentaacyl 4′-monophosphoryl lipid A samples from *S. minnesota* assuming at 40°C a cubic and at 70°C a H_{II} structure ([23] and own unpublished results). Furthermore, their acyl chain order does not differ significantly from that of '506'. In these terms, similar molecular conformation and acyl chain order,

the lower biological activities [11,12] of '504' and '505' cannot be understood. The only striking difference between the mono- and the diphosphoryl samples as observed here is the ester carbonyl hydration being much lower for the latter. An explanation for differences in biological response could also be the lower charge for the monophosphoryl samples which changes the 'solubility' of the lipids, i.e., leads to differences in aggregate size and stability, but also to a smaller value of the CAC and, with that, to a much smaller number of monomers/oligomers at a given concentration.

It should be noted that compound '406', which does not induce cytokines in human cell lines, may act as a potent antagonist of endotoxin by suppressing biological response completely when added in molar excess to LPS [4,52,53]. However, it was found that in murine-derived macrophages, it may act also as relatively strong agonist with an activity being one order of magnitude lower than LPS [54,55]. This discrepancy is surprising when considering that other antagonists like lipid A from *Rhodobacter sphaeroides* have this property independently of the cellular system selected.

Anyway, the prerequisite for the antagonistic action of lipid A-like structures should be the cylindrical conformation of individual molecules leading in aggregated form to a lamellar supramolecular structure and the existence of a sufficient number of 3-OH acyl chains. This could lead to peculiar intra- and intermolecular conformations of single groups like the phosphates (Fig. 7c) contrasting with the spectral pattern of agonistic compounds. In this context, the spectral behaviour of lipid A from *Rhodobacter capsulatus*, exhibiting similar antagonistic potency as '406', should be mentioned. This lipid A gives rise to a very similar spectrum as '406' in the range 1320 to 1180 cm^{-1} with the highest intensity band components corresponding to very high hydration and nearly no component corresponding to low hydration of the phosphate groups (own unpublished results). It has, moreover, only one 3-OH group but two further 3-oxo groups. Therefore, a closer characterization of these and other potent antagonists should be important (lipid A from *Rh. sphaeroides* has two hydroxy and one oxo group, [56]).

Many biological processes are influenced by the acyl chain order [57], which can be roughly estimated by the peak positions of $\nu_s(CH_2)$. It may be assumed that biological action/activity may be enhanced for more unordered acyl chains to facilitate interaction with, e.g., target cell membranes. As the acyl chain order, however, is similar for compounds '504', '505', '506', and '516', whereas distinct differences are observed with respect to their ability to induce cytokines in macrophages, there is no direct correlation of biological activity to acyl chain order. This implies that, in accordance with recent findings for different LPS with varying sugar chain lengths or in different salt forms [21–23], a low acyl chain order is not a priori a prerequisite for biological activity.

Acknowledgements

References

[1] E.Th. Rietschel, T. Kirikae, F.U. Schade, U. Mamat, G. Schmidt, H. Loppnow, A.J. Ulmer, U. Zähringer, U. Seydel, F. Di Padova, M. Schreier, H. Brade, FASEB J. 8 (1994) 217–225.

[2] E.Th. Rietschel, H. Brade, O. Holst, L. Brade, S. Müller-Loennies, U. Mamat, U. Zähringer, F. Beckmann, U. Seydel, K. Brandenburg, A.J. Ulmer, T. Mattern, H. Heine, J. Schletter, S. Hauschildt, H. Loppnow, U. Schönbeck, H.-D. Flad, U.F. Schade, F. Di Padova, S. Kusumoto, R.R. Schumann, Curr. Top. Microbiol. Immunol. 216 (1995) 39–81.

[3] T. Lüderitz, K. Brandenburg, U. Seydel, A. Roth, C. Galanos, E.Th. Rietschel, Eur. J. Biochem. 179 (1989) 11–16.

[4] H. Loppnow, H.-D. Flad, E.Th. Rietschel, H. Brade, In: G. Schlag, H. Redl (Eds.), Pathophysiology of Shock, Sepsis, and Organ Failure, Springer-Verlag, Berlin, 1995, pp. 405–416.

[5] H. Loppnow, P. Libby, M. Freudenberg, J.H. Krauss, J. Weckesser, H. Mayer, Infect. Immun. 58 (1990) 3743–3750.

[6] E.Th. Rietschel, L. Brade, O. Holst, V.A. Kulshin, B. Lindner, A.P. Moran, U.F. Schade, U. Zähringer, H. Brade, In: A. Nowotny, J.J. Spitzer, E.J. Ziegler (Eds.), Cellular and Molecular Aspects of Endotoxin Reactions, Elsevier, Amsterdam, 1990, pp. 15–32.

[7] M. Imoto, N. Yoshimura, S. Kusumoto, T. Shiba, Proc. Jpn. Acad. Ser. B 60 (1984) 285–288.

[8] N. Kasai, S. Arata, J.-I. Mashimo, K. Okuda, Y. Aihara, S. Kotani, H. Takada, T. Shiba, S. Kusumoto, M. Imoto, H. Yoshimura, T. Shimamoto, Infect. Immun. 51 (1986) 43–48.

[9] C. Galanos, O. Lüderitz, M. Freudenberg, L. Brade, U. Schade, E.Th. Rietschel, S. Kusumoto, T. Shiba, Eur. J. Biochem. 160 (1986) 55–59.

[10] S. Kotani, H. Takada, I. Takahashi, M. Tsujimoto, T. Ogawa, T. Ikeda, K. Harada, H. Okamura, T. Tamura, S. Tanaka, T. Shiba, S. Kusumoto, M. Imoto, H. Yoshimura, N. Kasai, Infect. Immun. 52 (1986) 872–884.

[11] E.Th. Rietschel, L. Brade, U. Schade, U. Seydel, U. Zähringer, H. Loppnow, H.-D. Flad, H. Brade, In: G. Gregoridias, A.C. Allison, G. Poste (Eds.), Immunological Adjuvants and Vaccines, Plenum press, New York, 1989, pp. 61–74.

[12] H. Takada, S. Kotani, CRC Crit. Rev. Microbiol. 16 (1989) 477–523.

[13] C. Galanos, O. Lüderitz, E.Th. Rietschel, O. Westphal, H. Brade, L. Brade, M. Freudenberg, U. Schade, M. Imoto, H. Yoshimura, S. Kusumoto, T. Shiba, Eur. J. Biochem. 148 (1985) 1–5.

[14] K. Brandenburg, M.H.J. Koch, U. Seydel, J. Struct. Biol. 105 (1990) 11–21.

[15] U. Seydel, K. Brandenburg, M.H.J. Koch, E.Th. Rietschel, Eur. J. Biochem. 186 (1989) 325–332.

[16] U. Seydel, K. Brandenburg, In: D.C. Morrison, J. Ryan (Eds.), Bacterial Endotoxic Lipopolysaccharides, CRC Press, Bota Racon, 1992, pp. 225–250.

[17] K. Brandenburg, U. Seydel, In: R.E. Hester, R.B. Girling (Eds.), Spectroscopy of Biological Molecules, Bookcraft, Bath, 1991, pp. 191–192.

[18] K. Brandenburg, Biophys. J. 64 (1993) 1215–1231.

[19] J.N. Israelachvili, S. Marcelja, R.G. Horm, Q. Rev. Biophys. 13 (1980) 121–200.

[20] J.N. Israelachvili, Intermolecular and Surface Forces, Academic Press, London, 1991, pp. 366–394.

[21] U. Seydel, H. Labischinski, M. Kastowsky, K. Brandenburg, Immunobiol. 187 (1993) 191–211.

[22] K. Brandenburg, H. Mayer, M.H.J. Koch, J. Weckesser, E.Th. Rietschel, U. Seydel, Eur. J. Biochem. 218 (1993) 555–563.

[23] K. Brandenburg, A.B. Schromm, M.H.J. Koch, U. Seydel, In: J. Levin, C.R. Alving, R.S. Munford, H. Redl (Eds.), Bacterial Endotoxins: Lipopolysaccharides from Genes to Therapy, Wiley, New York, 1995, pp. 167–182.

[24] S. Kusumoto, M. Inage, H. Chaki, M. Imoto, T. Shimamoto, T. Shiba, In: L. Anderson, F.M. Unger (Eds.), Bacterial Lipopolysaccharides: Structure, Synthesis, and Biological Activities, American Chemical Society, Washington DC, 1983, p. 237.

[25] M. Imoto, H. Yoshimura, T. Shimamoto, N. Sakaguchi, S. Kusumoto, T. Shiba, Bull. Chem. Soc. Jpn. 60 (1987) 2205–2214.

[26] M. Imoto, H. Yoshimura, M. Yamamoto, T. Shimamoto, S. Kusomoto, T. Shiba, Bull. Chem. Soc. Jpn. 60 (1987) 2197–2204.

[27] J.K. Kauppinen, D.J. Moffat, H.H. Mantsch, D.G. Cameron, Appl. Spectrosc. 35 (1981) 271–276.

[28] M.H.J. Koch, J. Bordas, Nucl. Instr. Meth. 208 (1983) 461–469.

[29] A. Gabriel, Rev. Sci. Instrum. 48 (1977) 195–200.

[30] C. Tanford, The Hydrophobic Effect, Wiley, New York, 1980.

[31] H.H. Mantsch, R.N. McElhaney, Chem. Phys. Lipids 57 (1991) 213–226.

[32] U. Seydel, K. Brandenburg, E.Th. Rietschel, Prog. Clin. Biol. Res. 388 (1994) 17–30.

[33] K. Brandenburg, M.H.J. Koch, U. Seydel, J. Struct. Biol. 108 (1992) 93–106.

[34] U. Seydel, M.H.J. Koch, K. Brandenburg, J. Struct. Biol. 110 (1993) 232–243.

[35] I.M. Helander, L. Hirvas, J. Tuominen, M. Vaara, Eur. J. Biochem. 204 (1992) 1101–1106.

[36] K. Takayama, D.H. Mitchell, Z.Z. Din, P. Mukerjee, C. Li, D.L. Coleman, J. Biol. Chem. 269 (1994) 2241–2244.

[37] A.B. Schromm, K. Brandenburg, E.T. Rietschel, U. Seydel, J. Endotox. Res. 2 (1995) 313–323.

[38] U.P. Fringeli, H.H. Günthard, In: E. Grell (Ed.), Membrane Spectroscopy, Springer-Verlag, Berlin, 1981, pp. 270–332.

[39] P.M. Green, J.T. Mason, T.J. O'Leary, I.W. Levin, J. Phys. Chem. 91 (1987) 5099–5103.

[40] J.R. Silvius, Lipid Protein Interact. 2 (1982) 239–281.

[41] K. Brandenburg, U. Seydel, Eur. Biophys. J. 16 (1988) 83–94.

[42] K. Brandenburg, U. Seydel, Biochim. Biophys. Acta 775 (1984) 225–238.

[43] D. Naumann, C. Schultz, A. Sabisch, M. Kastowsky, H. Labischinski, J. Molec. Struct. 214 (1989) 213–246.

[44] H. Labischinski, G. Barnickel, H. Bradaczek, D. Naumann, E.Th. Rietschel, P. Giesbrecht, J. Bacteriol. 162 (1985) 9–20.

[45] M. Kastowsky, A. Sabisch, T. Gutberlet, H. Bradaczek, Eur. J. Biochem. 197 (1991) 707–716.

[46] G. Emmerling, U. Henning, T. Gulik-Krzywicki, Eur. J. Biochem. 78 (1977) 503–509.

[47] E.Th. Rietschel, H. Brade, Sci. Am. 267 (1992) 54–61.

[48] D. Naumann, C. Schultz, J. Born, H. Labischinski, K. Brandenburg, G. von Busse, H. Brade, U. Seydel, Eur. J. Biochem. 164 (1987) 159–169.

[49] H. Labischinski, D. Naumann, C. Schultz, S. Kusumoto, T. Shiba, E.Th. Rietschel, P. Giesbrecht, Eur. J. Biochem. 179 (1989) 659–665.

[50] E.Th. Rietschel, L. Brade, K. Brandenburg, H.-D. Flad, J. de Jong-Leuveninck, K. Kawahara, B. Lindner, H. Loppnow, T. Lüderitz, U. Schade, U. Seydel, S. Sidorzyk, A. Tacken, U. Zähringer, H. Brade, Rev. Infect. Dis. 9 Suppl. 5 (1987) 527–536.

[51] E.Th. Rietschel, L. Brade, U. Schade, C. Galanos, M. Freudenberg, O. Lüderitz, S. Kusumoto, T. Shiba, Eur. J. Biochem. 169 (1987) 27–31.

[52] M.-H. Wang, W. Feist, H. Herzbeck, H. Brade, S. Kusumoto, E.Th. Rietschel, H.-D. Flad, A.J. Ulmer, FEMS Microbiol. Immunol. 64 (1990) 179–186.

[53] A.J. Ulmer, T. Mattern, H. Heine, B. Weidemann, H. Brade, E.Th. Rietschel, H.-D. Flad, In: D.C. Morrison, J.L. Ryan (Eds.), Novel Therapeutic Strategies in the Treatment of Sepsis, Marcel Dekker, New York, 1996, pp. 133–147.

[54] D.T. Golenbock, R.Y. Hampton, N. Qureshi, K. Takayama, C.R.H. Raetz, J. Biol. Chem. 266 (1991) 19490–19498.

[55] K.-J. Tanamoto, J. Immunol. 155 (1995) 5391–5396.

[56] N. Qureshi, J.P. Honovich, H. Hara, J.C. Cotter, K. Takayama, J. Biol. Chem. 263 (1988) 5502–5504.

[57] R.C. Aloia, Membrane Fluidity in Biology, Vol. 1 and 2, Academic Press, New York, 1983.